

Fabrication of 1-dimensional porous hydroxyapatite and evaluation of its osteoconductivity

HYUN-SEUNG RYU, SU-JIN KIM, JIN-HO KIM, HWAN KIM, KUG SUN HONG*
School of Materials Science and Engineering, College of Engineering, Seoul National University, Shinrim-dong, San 56-1, Kwanack-Ku, Seoul, Korea, 151-742
E-mail: kshongss@plaza.snu.ac.kr

BONG-SUN CHANG, DONG-HO LEE, JAE HYUP LEE, CHOON-KI LEE
Department of Orthopedic Surgery, College of Medicine, Seoul National University, Yungun-dong 28, Chongno-Ku, Seoul, Korea, 110-744

SUNG-SOO CHUNG
Department of Orthopedic Surgery, College of Medicine, Sung Kyun Kwan University, Ilwon-dong 50, Kangnam-Ku, Seoul, Korea, 135-230

Porous HA ceramics with 1-dimensional pore channels were fabricated to obtain controllable microstructure. 1-dimensional porous HA was objected to find out the optimum condition of bone ingrowth and also to facilitate the observation of osteoconductive behavior in porous HA. The porous structure was formed by burnt-out of polymeric fibers and the size of pores was determined by the diameter of polymeric fibers. The porosity could be varied by the thickness of HA slurry coated on polymeric fiber and by the thickness of HA tapes inserted between fiber layers. As result, 1-dimensional porous HA ceramics of this study have the uniform interconnection size (50–500 μm) and the linearly open pore structure. The compressive strength of 1-dimensional porous HA was 6–10 MPa similar to that of human cancellous bone. On the *in vivo* test, oteon-like osteoconduction in pore channel of 1-dimensional porous HA was observed, like what had been found in cortical bones. This osteon-like new bone grew from the surface to the center of pore channels. The 1-dimensional porous HA ceramics prepared in this study were very useful as a model system to observe bone ingrowth in the porous HA implants.

© 2004 Kluwer Academic Publishers

1. Introduction

Calcium hydroxyapatite [$\text{Ca}_{10}(\text{PO}_4)_6(\text{OH})_2$] is a major part of inorganic components of natural bone [1] and synthesized HA makes bonding interfaces with bone in body [2,3], which has strongly suggested the applicability of synthesized HA in bone replacement. However, in applications of HA in the form of dense ceramic body, it is difficult to obtain bone ingrowth into dense ceramics, therefore resulting weak bonding with bone [4]. Moreover, HA bone graft remains in the body for a long term due to its poor biodegradability [5].

Biphasic composites of HA and biodegradable material, i.e. HA/TCP has been studied as an alternative to dense HA ceramics [6,7]. However, it is difficult to match the bioresorption rate with the rate of bone ingrowth or to make degraded parts have 3-dimensionally interconnected structure to allow continuous bone ingrowth.

Porous HA ceramics are expected to overcome

limitations of dense HA or HA/TCP ceramics [8]. This consists of HA skeleton and porous parts to accommodate bone to grow into. Various preparation methods of porous HA ceramics has been reported. Firing below the sintering temperatures [9,10] or burning out polymer bead or naphthalene incorporated into HA mixture has been utilized most frequently to obtain porous body [11,12]. In these methods, while the porosity can be easily controlled by changing firing temperatures or amount of additives, isolated pores or if interconnected, pores of small interconnection size are usually formed, which will obstruct bone ingrowth.

To obtain good bone growth, 3-dimensionally interconnected structure of pores are essential and the size of interconnection is a more important factor than the pore size itself [13]. This interconnected structure can be obtained by using polymeric sponge [8,14]. Polyurethane sponge that was imbedded into HA slurry is dried and fired remaining 3-dimensionally intercon-

*Author to whom all correspondence should be addressed.

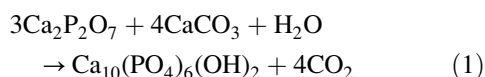
nected HA ceramic skeleton that will be sintered. The resulting porous HA ceramics have broad range of interconnection size and random distribution of pores. These features and the possibility of blocked pores by extra HA slurry limit the potential as a model for study of bone growth for purpose to determine the optimum interconnection size, porosity or pore configuration.

For this purpose, a new type of porous body is required. Porous body containing parallel arrangement of 1-dimensional pores can give uniform size and shape of pores, continuous path for bone growth, which will allow systematic study of osteoconduction after implant by observing cross-section. In this study, 1-dimensionally porous HA ceramics were fabricated and their pore size and porosity could be controlled. The compressive strength was measured and the feature of bone in-growth was compared with the case of 3-dimensionally (3-D) porous HA bodies prepared by polymeric sponge method.

2. Experimental procedures

2.1. HA powder preparation

HA powder was synthesized through the solid-state reaction. Starting materials were $\text{Ca}_2\text{P}_2\text{O}_7$, heat-treated from $\text{CaHPO}_4 \cdot 2\text{H}_2\text{O}$ (Junsei Co, Japan) at 1100°C , and CaCO_3 (High Purity Chemical, Japan). $\text{Ca}_2\text{P}_2\text{O}_7$ and CaCO_3 were weighed to be 1.67 of Ca/P ratio and mixed with ZrO_2 balls in anhydrous ethanol media. Dried mixed powder was calcined at 1100°C for 12 h to be pure HA by the Equation 1. On the phase analysis with powder X-ray diffractometer (XRD; Model M18XHF, Mac science instruments, Japan), no secondary phases or unreacted species were detected.



Synthesized HA powder was ball-milled for 24 h and the particle size of final powder was $1.5\text{--}2\ \mu\text{m}$

2.2. HA tape casting

HA powder was ball-milled in nonaqueous solvent for 24 h. Plasticizer and binder were added to the ball-milled slurry. The HA slurry was de-aired under the vacuum for the easy control of viscosity and for the removal of bubbles. The obtained HA slurry was spread by means of a doctor blade on the Mylar film. The blade gap was $100\text{--}200\ \mu\text{m}$ and the feed speed was $5\ \text{mm/s}$. The HA tape was dried at the room temperature in the clean room to avoid the contamination. No crack was observed in the HA.

2.3. Fabrication of sponge-type porous bodies

For the comparative study with the case of 1-dimensionally porous HA ceramics, sponge-type porous HA bodies were prepared. As reported by several researchers [8, 14], $300\text{--}500\ \mu\text{m}$ pore-sized polyurethane sponges were imbedded in HA aqueous slurry containing PVA

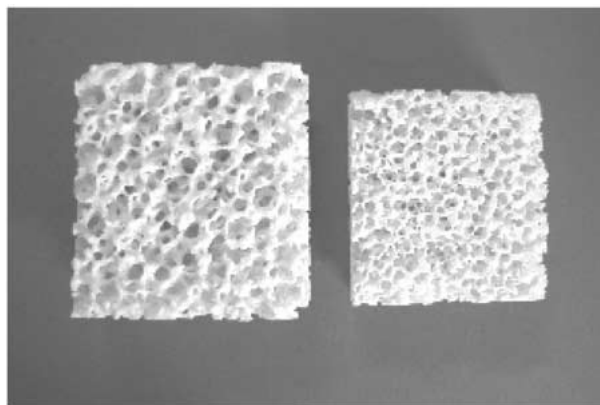


Figure 1 Sponge type 3-dimensional porous HA.

binder, and excess HA slurry was removed. Dried specimens were heat-treated at 600°C to burn out all polymer species and sintered at 1300°C for 2 h. ‘‘Sponge’’ type porous HA ceramics, thus produced, was presented in Fig. 1.

2.4. In vivo test

One-dimensionally porous HA bodies of four different sizes of interconnection and one kind of sponge-type HA samples were machined into blocks of $5 \times 5 \times 7\ \text{mm}^3$ and sterilized by EO gas before implantation. Specimens of each type of porous HA bodies were inserted to the cortical window made on the proximal tibiae of rabbits (mature male New Zealand rabbits weighing about $3.5\ \text{kg}$). After 8 weeks, the rabbits were sacrificed for the observation of bone in-growth by the light microscopy and SEM (Model JSM-5600, Jeol, Japan) examination.

3. Results and discussion

3.1. Process of 1-dimensional porous HA fabrication

Porous HA ceramics of 1-dimensional pore structure were fabricated by the process as shown in Fig. 2. First, polymeric fiber of proper diameter was prepared and HA slurry for tape casting was coated on polymeric fiber in order to prevent collapse of pores by separating the fibers. HA coating on polymeric fiber was achieved by passing polymeric fiber through viscosity-controlled HA slurry at $1\text{--}5\ \text{m/min}$ and by drying quickly in the hot zone of vertical electric furnace at the temperature near 150°C . HA coated fibers were arranged compactly on as-prepared HA tape and the voids among fibers and HA tape were filled with HA slurry. On that layer, another HA tape was laid. After drying the sheet at the room temperature, each layer was cut from the whole sheet and stacked to the required size and thickness. Stacked HA-coated fiber layers were laminated under the pressure at 120°C . Non-aqueous solvent was evaporated and binder was thermally hardened. The formed green body was sintered through 2-step heating process: for the complete oxidation of polyester fiber, binder, plasticizer and residue polymer and slow evaporation of overall polymer, the temperature was raised to 600°C at the low heating rate (1°C/min); then was raised to 1300°C at

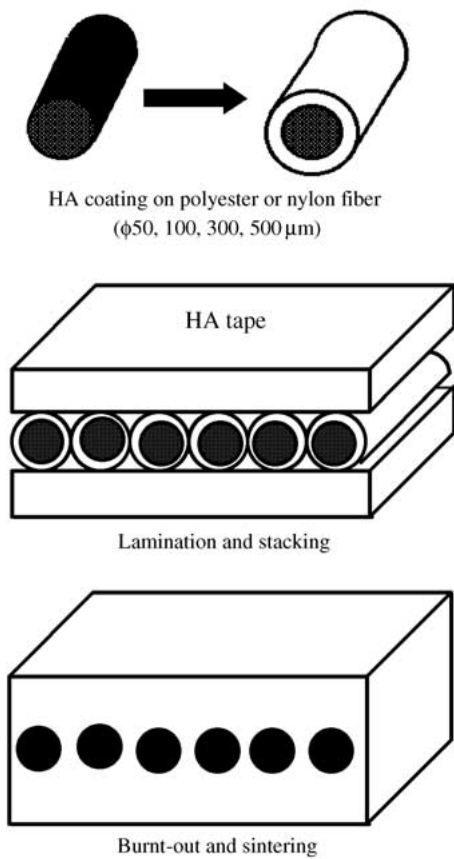


Figure 2 Preparation of 1-dimensional porous HA.

the rapid heating rate (5 °C/min), followed by holding at 1300 °C for 2 h. The space that had been occupied by polymeric fiber was turned into macro-pore and the porous HA body with linear pores was fabricated.

3.2. Control of pore size and porosity

The pore size of these porous HA bodies could be determined by the diameter of polyester fiber that burnt-out during the heating process. The pore geometry is the shape of pipe of uniform cross section and in this case the pore size equals the interconnection size. Fig. 3 shows 1-dimensionally porous HA specimens of various interconnection size which were prepared using polymeric fibers of different diameters. In this study, 1-dimension porous HA ceramics of 50–500 μm pore size were fabricated, according to the report by Hulbert *et al.* that bone ingrowth could take place in the specimen having pores of at least 100 μm size [15].

Porosity of 1-dimension porous HA is controlled by three parameters: (1) the diameter of polymeric fiber; (2) the thickness and frequency of HA tape layer inserted between fiber layers; and (3) the thickness of HA coating on fiber or the separation between adjacent fibers. If pores were formed only by burning-out of polymeric fibers, porosity would be determined by the Equations 1 and 2 according to these parameters.

$$\rho = \frac{m}{V} = \frac{(4(t + R_f + R_c) \times (R_f + R_c) - \pi \times R_f^2)}{4(t + R_f + R_c) \times (R_f + R_c)} \times 100(\%) \quad (2)$$

$$\text{porosity } (\%) = 100 - \frac{\rho}{3.156} \times 100 \quad (3)$$

where ρ : density, m : mass, V : volume, R_f : fiber radius, R_c : fiber radius + HA coating thickness, t : HA tape thickness.

Assuming closed packing of uncoated fibers, the

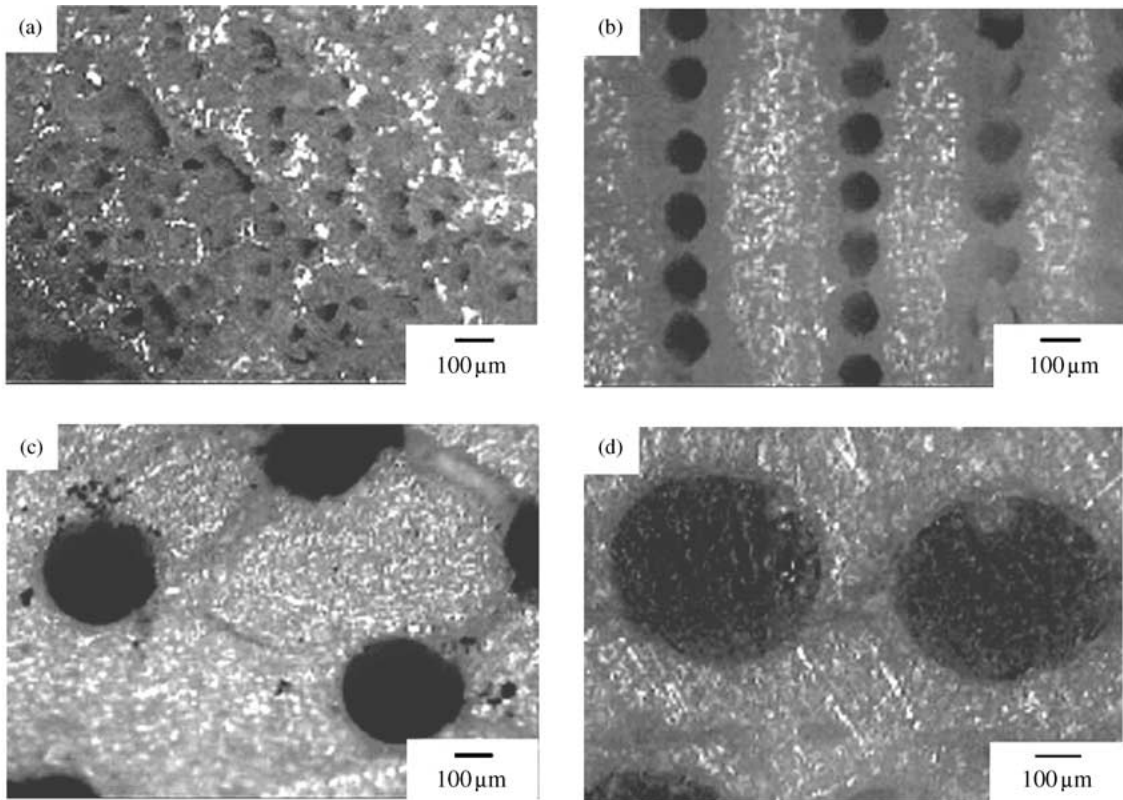


Figure 3 Pore (interconnection) size of 1-dimensional porous HA: (a) φ50 (μm), (b) φ100μm, (c) φ300μm, (d) φ500μm.

porous HA would have the maximum porosity of 90.0%, therefore, ideally, porosity of 0–90% can be obtained.

Fig. 4 shows the result of porosity control by the frequency of HA tape insertion into layers of polymeric fiber of 100 μm diameter: (a) one HA tape per one fiber layer giving 25% porosity, (b) two HA tapes per three polymeric fiber layers having 50% porosity, (c) no HA tape resulting 65% porosity. The maximum porosity of 1-dimension porous HA body could be obtained in case of no intervening HA tape, and in the case of 100 μm pore size, 65% is the maximum porosity. This value is lower than 90%, the theoretically calculated maximum porosity with Equation 1, due to the space between fiber layers incorporated to prevent the collapse of 1-dimension pore structure.

The viscosity of HA slurry affects thickness of HA coating layer on polymeric fiber. HA coating slurry was

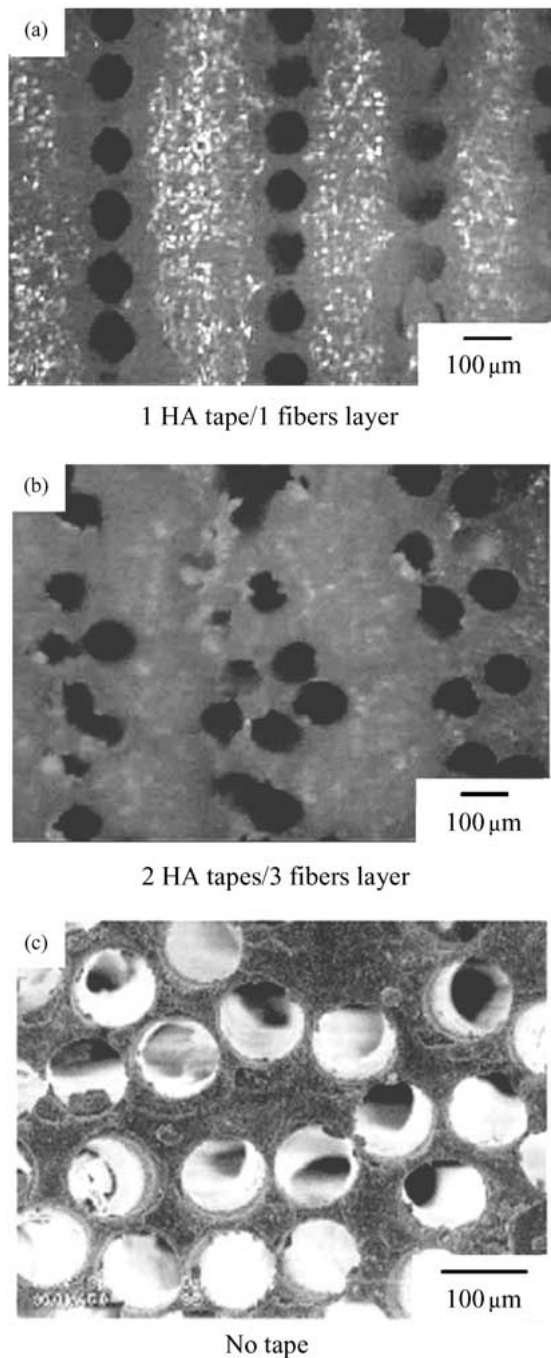


Figure 4 Porosity control of 1-dimensional porous HA (HA tape).

consisted of HA powders, nonaqueous solvent, plasticizer, and binder. The viscosity of coating slurry was controlled by changing the volume percent of nonaqueous solvent, which was achieved by evaporation in vacuum chamber. Fig. 5(a) shows the viscosity change with the de-airing time and (b) represents the thickness change with the viscosity of HA coating slurry. The maximum uniform coating thickness that could be achieved in this study was 120 μm and above 120 μm HA coating layer leaned to one side from the center of fiber. Fig. 5(c) shows the plot of density and porosity of 1-dimension porous HA with the thickness of HA coating layer, compared with the values calculated with Equation 1. Porosity decreased with increasing HA coating thickness. The difference between theoretical value and measured value was originated from micro-cracks during burning out polymeric fibers. In addition, the effect of HA coating thickness was more significant in case of larger diameter of polymeric fiber, because the area of pore increases with the square of pore size.

Table I presents porosity of 1-dimensional porous HA having various pore sizes. In Table I, a macropore means pore formed by burning out polymeric fiber and

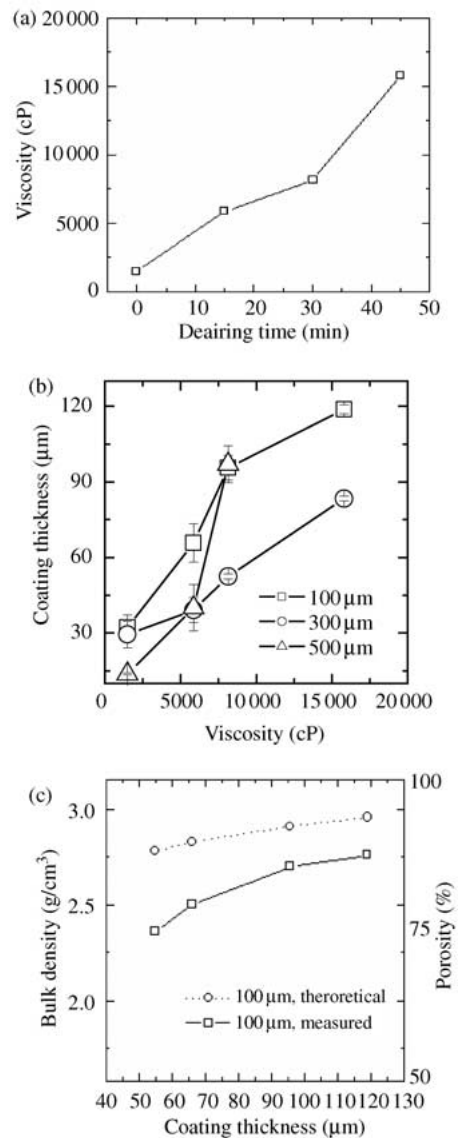


Figure 5 Porosity control of 1-dimensional porous HA (HA coating thickness).

TABLE I Interconnection size, porosity and compressive strength of 1-dimensional porous HA

Notation	Measured interconnection size (μm)	Macroporosity (%)	Total porosity (%)	Compressive strength (MPa)
1D-50	49.3 ± 1.63	12.9 ± 0.79	42.3 ± 0.47	12.7 ± 1.36
1D-100	94.1 ± 1.28	20.3 ± 3.96	49.9 ± 2.72	6.12 ± 2.02
1D-300	272.4 ± 5.4	23.6 ± 1.63	42.1 ± 2.83	7.98 ± 1.66
1D-500	472.2 ± 8.2	32.8 ± 1.81	47.3 ± 1.97	10.3 ± 3.58
3D-300 (Sponge)	250 ± 5.0	—	83.9 ± 2.31	0.19 ± 0.07

micropore means undesirable pore originated from cracks between layers, flaws, or from evaporation of organic components in HA tapes or coating layers. The total porosity that is the macroporosity added with the microporosity was 40–50% and the discrepancy between the measured value and the calculated one was relatively small in the porous HA of larger pore size. This is due to the fact that volume portion of fibers increases with the diameter, increasing the macroporosity. On the other hand, the porosity of 3-dimensional porous HA prepared by the sponge method was near 80%, which was higher than that of 1-dimensional porous HA having pipe-type pores, since pores of 3-dimensional porous HA interconnected randomly and kept open cell structure. If it were attempted to reduce porosity of 3-dimensional porous HA, excess HA slurry would close open pore. Therefore considering porosity 1-dimensional porous HA have medium value of porosity compared with porosity of dense HA and 3-dimensional porous HA. The compressive strength of 1-dimensional porous HA ceramic specimen was 6–10 MPa that is similar with that of human cancellous bone [16]. This is much higher than that of 3-dimensional porous HA ceramic body, 0.2 MPa, due to relatively low porosity of 1-dimensional porous HA ceramics. In Fig. 6, the observed stress/strain curve was shown. The result did not show abrupt fracture characteristic of brittle ceramics, which may be attributed to hindrance of crack propagation by HA tape inserted between fiber layers.

3.3. Osteoconduction in 1-dimension porous HA ceramics

We observed osteoconduction in 1-dimensional porous HA ceramics implanted into proximal tibia of rabbits. Compared with irregular woven bone structure in the

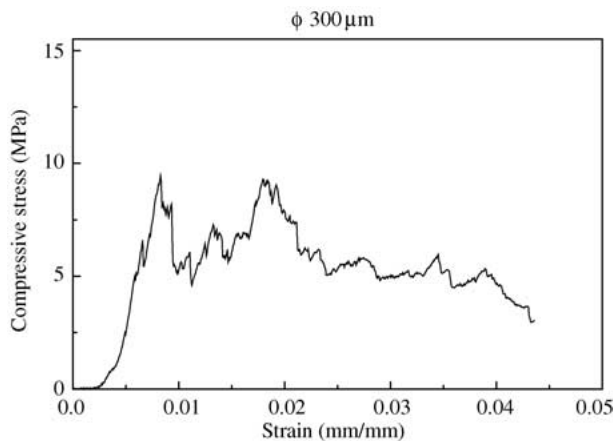
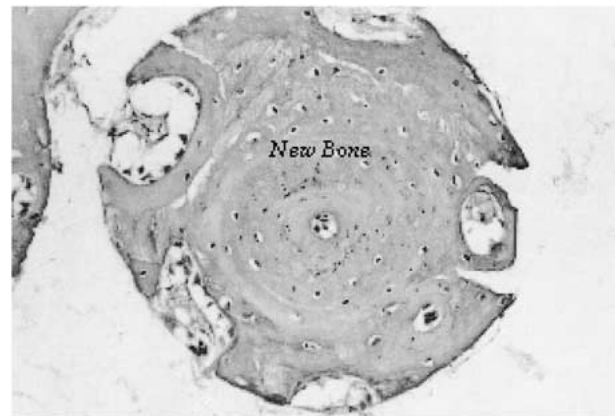
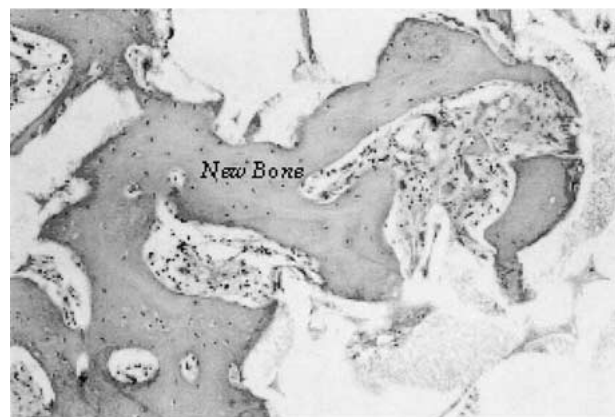


Figure 6 The stress and strain curve of 1-dimensional porous HA (1D-300).

case of sponge-like 3-dimensional porous HA ceramics (Fig. 7(b)), bone ingrowth in 1-dimensional porous HA ceramics took the concentric circular shape, which was similar with osteon structure as observed in cortical bone (Fig. 7(a)). Fig. 8(a) shows the back scattered scanning electron microscopy (BSSEM) micrograph of the cross section of a linear pore channel in the specimen. New bone had grown into the implant from the opening of pore to the center of pore channel, and the existence of blood vessel at the center of pore can be noticed. Fracture took place inside the ceramics, not at the interface between bone and ceramics, indicating strong chemical bonding with bone. The osteoconduction model inferred from the above findings, is illustrated schematically in Fig. 8(b) and as follow: blood vessel grows along the center of pore channel; osteocytes anchor on the surface of pore channel; new bone formation extends into the inner space; osteocytes are generated on the surface of new bone and so on. This model can explain the observation that bone grows most actively at the entrance



(a)

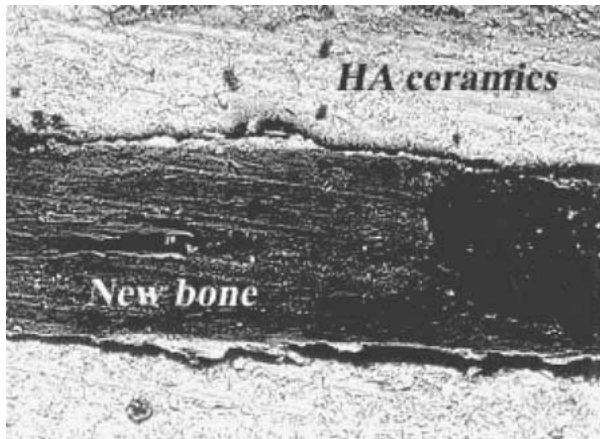


(b)

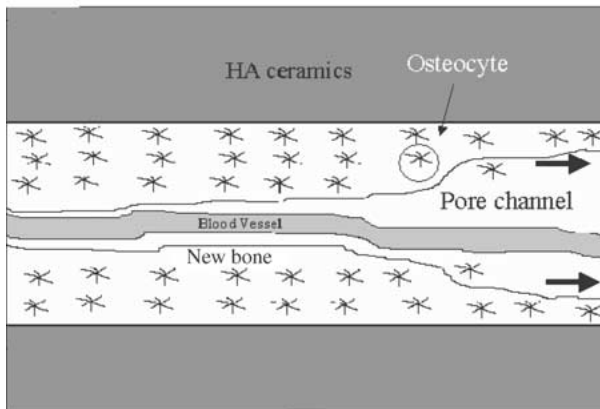
Figure 7 Optical microscopy results: (a) 4 weeks, 1D-300, $\times 120$, (b) 4 weeks, 3D-300, $\times 120$.

TABLE II Comparison of osteoconduction on *in vivo* test of 1-dimensional and 3-dimensional porous HA

	4 weeks	8 weeks	Compressive strength
1-Dimensional porous HA	Osteon structure	*Remodeling of new bone and bone marrow formation	High compressive strength
3-Dimensional porous HA	Irregular woven bone structure	*Significantly increased mechanical strength after implantation	Flexible and ductile



(a)



(b)

Figure 8 (a) Back scattering SEM of longitudinally cut, 1D-300 specimen at 8 week; magnification: $\times 200$, (b) Schematic illustration of the osteoconduction of 1D-300 specimen.

of pore channel and that bone growth into the pore channel slows down. This feature of new bone formation could not be observed in many other studies with 3-dimensional porous specimens.

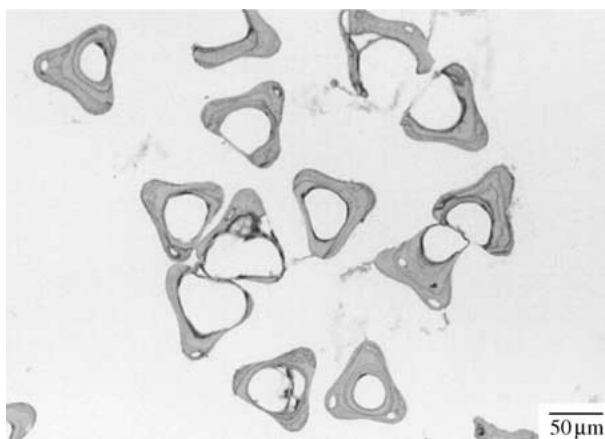


Figure 9 Optical microscopy results (1D-50 ($\phi 50\mu\text{m}$), 8 weeks after implantation).

Well-defined pore sizes in this study made it possible to observe osteoconduction in pores of various sizes. As shown in Fig. 9, osteoconduction was found in pore channel of $50\mu\text{m}$ diameter, in accordance with our previous report [17], which was contrary to previous reports of other groups that interconnection size must be larger than $100\mu\text{m}$ to accommodate new bone ingrowth.

The comparison of characteristics of osteoconduction in 1-dimensional porous HA ceramics and in 3-dimensional sponge type HA bodies are summarized in Table II.

4. Conclusions

In this study, porous HA ceramics with linear pore channels were fabricated to obtain controllable microstructure to find out the optimum condition of bone ingrowth and also to facilitate the observation of osteoconductive behavior in porous HA. Our 1-dimensional porous HA ceramics have the uniform interconnection size and the linearly open pore structure. The porous structure was formed by burnt-out of polymeric fibers and the size of pores was determined by the diameter of polymeric fibers. The porosity could be varied by the thickness of HA slurry coated on polymeric fiber and by the thickness of HA tapes inserted between fiber layers. On the *in vivo* test, osteoconduction in the osteon-like form was observed, like what had been found in cortical bones. This osteon-like forms extend from the specimen surface to the center of pore channels. The 1-dimensional porous HA ceramics prepared in this study were very useful as a model system to observe bone ingrowth in the porous HA implants.

Acknowledgments

This work was supported by a Grant-in-Aid for Next-Generation New Technology development Programs from the Korea Ministry of Commerce, Industry and Energy (No. N11-A08-1402-08-1-3). The authors thank to Bioalpha.com for technical assistance.

Reference

1. A. S. POSNER and F. BETTS, *Acc. Chem. Res.* **8** (1975) 273.
2. L. HONG, X. HENGCHANG and K. DE GROOT, *J. Biomed. Mater. Res.* **26** (1992) 7.
3. M. NEO, S. KOTANI, T. NAKAMURA, T. YAMAMURO, C. OHTSUKI, T. KOKUBO and Y. BANDO, *ibid.* **26** (1992) 1419.
4. M. JARCHO, *Clin. Orthop.* **157** (1981) 259.
5. N. KIVRAK and A. TAS CUNEY, *J. Am. Ceram. Soc.* **81** (1998) 2245.
6. J. WANG, W. CHEN, Y. LI, S. FAN, J. WANG and X. ZHANG, *Biomaterials* **19** (1998) 1387.
7. H. S. RYU, H. J. YOUN, K. S. HONG, S. J. KIM, D. H. LEE, B. S. CHANG, C. K. LEE and S. S. CHUNG, *Key Eng. Mater.* **218-220** (2002) 21.

8. X. YANG and Z. WANG, *J. Mater. Chem.* **8** (1998) 2233.
9. F. C. M. DRIESSENS, M. M. A. RAMSELAAR, H. G. SCHAEKEN, A. L. H. STOLS and P. J. VAN MULLEN, *J. Mater. Sci.: Mater. Med.* **3** (1992) 413.
10. K. YAMAMURA, H. IWATA and T. YOTSUYANAGI, *J. Biomed. Mater. Res.* **26** (1992) 1053.
11. R. E. HOLMES, R. W. BUCHOLZ and V. MONNEY, *J. Bone Joint Surg.* **71** (1986) 1487.
12. T. J. FLATLEY, K. L. LYNCH and M. BENSON, *Clin. Orthop.* **179** (1988) 246.
13. J. J. KLAWITTER and S. F. HULBERT, *J. Biomed. Mater. Res.* **2** (1971) 161.
14. J. SAGGIO-WOYANSKY, C. E. SCOTT and W. P. MINNEAR, *Am. Ceram. Soc. Bull.* **71** (1992) 1674.
15. S. F. HULBERT, S. J. MORRISON and J. J. KLAWITTER, *J. Med. Mater. Res.* **6** (1972) 347.
16. R. HOLMES, V. MOONEY, R. BUCHOLZ and A. TENCER, *Clin. Orthop. Res.* **183** (1984) 252.
17. B. S. CHANG, C. K. LEE, K. S. HONG, H. J. YOUN, H. S. RYU, S. S. CHUNG and K. W. PARK, *Biomaterials* **21** (2000) 1291.

*Received 20 May 2002
and accepted 7 August 2003*